

Longitudinal Spontaneous Polarization and Longitudinal Electroclinic Effect in Achiral Smectic Phases with Bent-Shaped Molecules

Arun Roy,¹ N. V. Madhusudana,² P. Tolédano,^{1,*} and A. M. Figueiredo Neto¹

¹*Instituto de Física, Universidade de São Paulo, CP 66318, 05315-970 São Paulo, SP, Brazil*

²*Raman Research Institute, C. V. Raman Avenue, Bangalore 560080, India*

(Received 15 September 1998)

The stable smectic configurations associated with achiral bent-shaped molecules are investigated theoretically. Five different configurations of the molecules within the layers are found, among which two possess a spontaneous longitudinal polarization, consistent with the $\hat{n} \rightarrow -\hat{n}$ symmetry. Under application of a longitudinal electric field these configurations can give rise to remarkable field effects, such as a three-state switching of the transverse polarization under alternating field, and a longitudinal electroclinic effect. [S0031-9007(99)08447-1]

PACS numbers: 61.30.Cz, 77.84.Nh

Recently, the possibility of obtaining macroscopically chiral liquid crystal phases by the spontaneous organization of achiral molecules was demonstrated experimentally [1,2]. Antiferroelectric smectic domains formed from molecules with bent cores that are achiral were obtained with two types of tilted configurations displaying alternate or uniform handedness from layer to layer [2]. The bent geometry of the molecules allows within the smectic layers a polar order perpendicular to the director. Subsequently the synthesis of a variety of liquid crystal compounds with “banana” shaped molecules was reported [3]. The aims of this Letter are (i) to investigate theoretically the stable molecular configurations within the layers which are associated with achiral bent-shaped molecules (or any achiral molecules permitting a transverse polar order) and (ii) to work out the related phase diagram, and disclosing the specific physical effects. More precisely, starting from the coupling of the two relevant symmetry breaking instabilities, which are the polar orientational ordering perpendicular to the director \hat{n} and the molecular tilt, we show the following:

(1) Five different stable layer configurations can be found, two among which give rise to a spontaneous polarization perpendicular to the smectic layers, consistent with the $\hat{n} \rightarrow -\hat{n}$ symmetry. The possible homogeneous and inhomogeneous structures of the corresponding smectic mesophases are discussed.

(2) Under application of a longitudinal electric field, only two configurations remain stable. This gives rise to remarkable effects, such as a three-state switching of the transverse polarization under alternating field, and a longitudinal electroclinic effect.

We start from a SmA phase of achiral symmetry $D_{\infty h}$, in which the bent molecules rotate freely around their long axes, defined as the line joining the two ends of the bent molecules [Fig. 1(a)]. The average direction of the long axes defines the director \hat{n} . As the medium is cooled we assume that a transition takes place to a phase in which the molecules pack efficiently to produce layers with a transverse polar order described by the polarization \vec{P} . The molecules may also have a tilted organization with respect to the layer normal, with unit vector \hat{k} . The tilt order can be described by the axial vector $\vec{\xi} = (\hat{n} \times \hat{k})$.

Because of the achiral symmetry of the SmA phase the two order parameters \vec{P} and $\vec{\xi}$ have distinct symmetries and are associated with independent mechanisms (instabilities), which do not give rise to a bilinear piezoelectric coupling, as for the chiral SmA – SmC* transition [4]. The covariant form of the homogeneous part of the free-energy density up to the fourth-degree terms in $\xi = |\vec{\xi}|$ and $P = |\vec{P}|$, and assuming an applied longitudinal field \vec{E} , is given by

$$F_h(\vec{\xi}, \vec{P}, \hat{n}, \hat{k}, \vec{E}) = \frac{a}{2} \xi^2 + \frac{b}{4} \xi^4 + \frac{\alpha}{2} P^2 + \frac{\beta}{4} P^4 + \delta_1 \xi^2 P^2 + c_1 (\vec{\xi} \cdot \vec{P})^2 + \frac{1}{2\chi_o} (\hat{n} \cdot \vec{P})^2 + \frac{1}{2\chi_1} (\hat{k} \cdot \vec{P})^2 + d_1 \xi^2 (\hat{n} \cdot \vec{P})^2 + d_2 \xi^2 (\hat{k} \cdot \vec{P})^2 + d_3 (\hat{n} \cdot \vec{P}) (\hat{k} \cdot \vec{P}) (\hat{n} \cdot \hat{k}) - \vec{E} \cdot \vec{P}, \quad (1)$$

where a, b, α, β , etc., are phenomenological coefficients. Taking into account the $\hat{n} \rightarrow -\hat{n}$ symmetry, we have the constraint $\hat{n} \cdot \vec{P} = 0$ and the longitudinal component of the polarization $P_z = P \xi \sin \Psi$, where Ψ is the angle between $\vec{\xi}$ and \vec{P} [Fig. 1(a)]. F_h reduces to

$$F_h(\xi, P, \Psi, E) = \frac{a}{2} \xi^2 + \frac{b}{4} \xi^4 + \frac{\alpha}{2} P^2 + \frac{\beta}{4} P^4 - \gamma_1 \xi^2 P^2 \cos 2\Psi + \delta \xi^2 P^2 - EP \xi \sin \Psi, \quad (2)$$

where $\delta = \delta_1 + \frac{1}{2}(c_1 + \frac{1}{2\chi_1})$ and $\gamma_1 = \frac{1}{2}(\frac{1}{2\chi_1} - c_1)$. In order to describe the layer stackings one needs to take into account the interaction between the layers, which is expressed in the inhomogeneous part F_i of the free-energy density:

$$F_i(\xi, P_t, \Psi, \varphi, \varphi', \theta) = P\xi \cos \theta \cos \Psi \left(\mu_1 \frac{\partial \varphi'}{\partial z} + \mu_2 \frac{\partial \varphi}{\partial z} \right) + \frac{1}{2} K_{33} \xi^2 \left(\frac{\partial \varphi'}{\partial z} \right)^2 + \frac{1}{2} K P_t^2 \left(\frac{\partial \varphi}{\partial z} \right)^2, \quad (3)$$

where φ and φ' are, respectively, the angles made by the transverse component \vec{P}_t of \vec{P} and $\vec{\xi}$ with the x axis [Fig. 1(a)]. θ is the tilt angle. The μ_1 and μ_2 terms are, respectively, the direct and inverse flexoelectric terms. The K_{33} term is the bending elastic energy, and the K term reflects an analogous distortion for P_t .

Let us first determine the stable molecular in-layer configurations in the absence of an electric field which requires us to consider only the homogeneous free-energy density $F_h(E = 0)$. Minimizing $F_h(E = 0)$ with respect to Ψ yields the equation of state

$$\frac{\partial F_h}{\partial \Psi} = 2\gamma_1 \xi^2 P^2 \sin 2\Psi = 0. \quad (4)$$

Equation (4) and the corresponding minimization of F_h , with respect to ξ and P , show that four distinct smectic configurations can be stabilized which are represented on the left hand side of Figs. 1(b)–1(e).

(I) For $\Psi = \pm \frac{\pi}{2}$ one gets an achiral layer structure of monoclinic symmetry C_S , represented in Fig. 1(b), in which the tilt plane (\hat{n}, \hat{k}) is a mirror plane containing the polarization \vec{P} . Each layer possesses a longitudinal component $P_z = \pm P\xi$, \vec{P} making an angle $(\frac{\pi}{2} - \theta)$ with \hat{k} ; i.e., the layer configuration is not invariant by the $\hat{k} \rightarrow -\hat{k}$ (up-down) symmetry, although it is invariant by the $\hat{n} \rightarrow -\hat{n}$ symmetry.

(II) For $\Psi = 0, \pi$, one has a transversely polarized tilted SmC^* type phase, of monoclinic chiral symmetry C_2 , with \vec{P} perpendicular to the tilt plane. The layer stacking may correspond to uniform ($\Psi = 0$) or alternate ($\Psi = 0, \pi$) handedness [Fig. 1(c)] consistent with the observations of Link *et al.* [2].

(III) For $P = \pm(-\frac{\alpha}{\beta})^{1/2}$ and $\xi = 0$, the stable configuration is that of the transversely polarized SmA type, with the achiral symmetry C_{2v} [Fig. 1(d)]. Hence, it is a biaxial phase with a transverse polar order.

(IV) For $\xi = \pm(-\frac{\alpha}{\beta})^{1/2}$ and $P = 0$, one obtains a standard SmC achiral layer configuration of symmetry C_{2h} , with no transverse polarization [Fig. 1(e)].

Another stable configuration can be found when higher power terms are considered in F_h , as, for example, the eighth-degree invariant $\gamma_2 \xi^4 P^4 \cos^2 2\Psi$. This configuration, denoted V, corresponds to an arbitrary value of Ψ , varying with temperature as $\cos 2\Psi = \frac{\gamma_1}{2\gamma_2 P^2 \xi^2}$. It is the most general configuration shown in Fig. 1(a), which has the chiral symmetry C_1 , and is associated with a longitudinal component of the polarization $P_z = P\xi \sin \Psi$.

The stacked structures of the mesophases corresponding to the preceding configurations are obtained by minimizing the total free energy $\Phi = \int (F_h + F_i) dz$ with respect

to the different variational parameters. Because of the achirality of the parent SmA phase, there are no Lifshitz gradient terms formed with the order-parameter components in the inhomogeneous free-energy density F_i . An

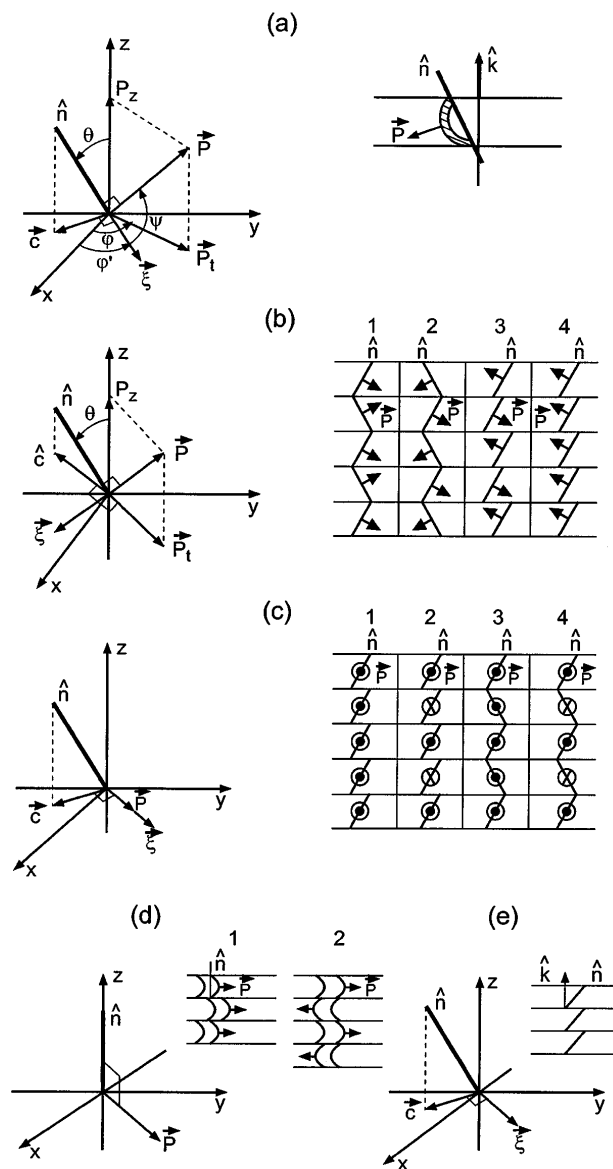


FIG. 1. Stable smectic configurations which can be exhibited by achiral bent molecules. (b)–(e) show the in-layer molecular configuration (left) and the corresponding possible layer stackings (right). The notation is defined in the text. (a) General triclinic configuration V; (b) achiral monoclinic configuration I; (c) transversely polarized SmC^* -type configuration II; (d) transversely polarized SmA -type configuration III; (e) SmC -type achiral configuration IV.

inhomogeneous (helical) ordering along the direction \hat{k} will be induced by the flexoelectric μ_1 and μ_2 invariants, which take nonzero values only in the configurations II and V and vanish in the configurations I, III, and IV. Hence, in the framework of our continuum model these latter configurations give rise only to homogeneous layered structures, which are represented on the right hand side of Figs. 1(b), 1(d), and 1(e). Four different stable layered structures are shown in Fig. 1(b) for the configuration I. The antiferroelectric structures (columns 2 and 3) are favored with respect to the ferroelectric structures (columns 1 and 4) by the packing constraints which try to make on the one hand the molecules to have the same bend directions within the same layer and on the other hand to have opposed bend directions in adjacent layers. Two different ferroelectric and antiferroelectric, layered structures are shown in Fig. 1(d) for the configuration III. The antiferroelectric structure is favored entropically, but it has been shown within a discrete model [5] that ferroelectric and helical structures can also be stabilized due to energetical considerations.

Assuming the same helicity for \hat{n} and \vec{P} , i.e., $\frac{\partial \varphi}{\partial z} = \frac{\partial \varphi'}{\partial z} = q$, where q is the helix wave vector, Ψ being independent of z , a minimization of the total free energy Φ with respect to q yields the equilibrium expression

$$q^e = -\frac{(\mu_1 + \mu_2)P^e \xi^e \cos \theta^e \cos \Psi^e}{K_{33}\xi^{e2} + K(1 - \xi^{e2} \sin^2 \Psi^e)}, \quad (5)$$

which shows that in the configurations I ($\cos \Psi^e = 0$), III ($\xi^e = 0$), and IV ($P^e = 0$) no helical order takes place. In contrast there exist two distinct types of inhomogeneous layer orderings corresponding to the configuration II [columns 1 and 4 in Fig. 1(c)], with homogeneously chiral layer structures, one of which (column 4) has been reported experimentally [3]. The other two [columns 2 and 3 of Fig. 1(c)] correspond to structures with racemic layer ordering. The configuration V gives rise to antiferroelectric or ferroelectric helical layer stackings similar to those for configuration II [Fig. 1(c)] with $0 < \Psi < \pi/2$ and differing by the property that the $\hat{k} \rightarrow -\hat{k}$ symmetry is not fulfilled.

Figures 2(a), 2(b), and 2(c) represent the regions of stability of the phases corresponding to the configurations I–V in the spaces of the phenomenological coefficients (α, a, γ_1) , $[(a - \alpha), \gamma_1]$, and (α, a) , respectively. One can see that phases I and II can be reached from the SmA phase only through phases III and IV, across two second-order transitions. The region of stability of phase V is located below the region of stability of phases I and II. The phase diagrams of Figs. 2(a) and 2(b) exhibit two four-phase points N_1 and N_2 at which merge the phases (I, II, III, V) and (I, II, IV, V), respectively.

Let us now disclose the effects resulting from the application of a longitudinal field. Assuming the flexoelectric contribution is small when $E \neq 0$, Eq. (4) is replaced by

$$\frac{\partial F}{\partial \Psi} = \xi P \cos \Psi (4\gamma_1 \xi P \sin \Psi - E) = 0. \quad (6)$$

Along with the equations minimizing $\Phi(E \neq 0)$ with respect to ξ and P , Eq. (6) shows that only two smectic configurations remain stable under applied field: (i) The achiral monoclinic configuration I, corresponding to $\Psi = \pm \frac{\pi}{2}$, which is stabilized for $E > E_{th}$ (for $\Psi = \frac{\pi}{2}$) or $E < -E_{th}$ ($\Psi = -\frac{\pi}{2}$), where E_{th} is a threshold field given by $E_{th} = 4\gamma_1 \xi^e P^e$, where ξ^e and P^e are the equilibrium values of ξ and P at zero field. The longitudinal component of the polarization is $P_z = \pm P^e \xi^e \xi_E^e$, where P^e and ξ_E^e are the equilibrium values of ξ and P in phase I in the presence of applied field $|\vec{E}| > E_{th}$. (ii) The general smectic configuration V corresponding here to $\sin \Psi = \frac{E}{E_{th}}$, which takes place for $-E_{th} \leq E \leq E_{th}$ and $\gamma_1 > 0$. The longitudinal component P_z is $P_z = \frac{E}{4\gamma_1}$ with $|E| < E_{th}$. Therefore, in the presence of a longitudinal electric field only the configurations displaying a longitudinal component of the polarization remain stable. Figure 2(d) shows the respective regions of stability of phases I and

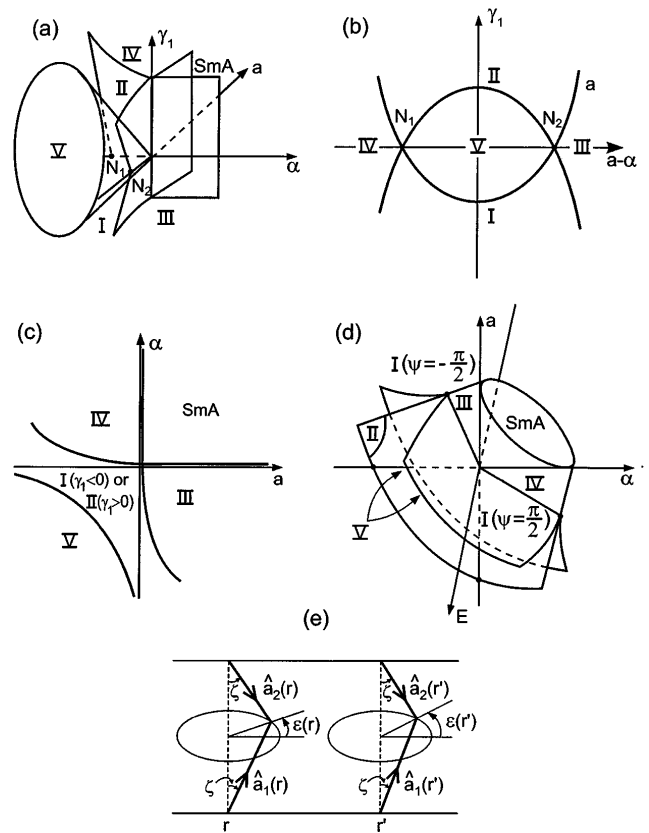


FIG. 2. (a)–(c) are phase diagrams at zero field $E = 0$ in the phenomenological parameter spaces (γ_1, α, a) , $(\gamma_1, a - \alpha)$, and (α, a) . The phases, denoted from I–V, are separated by second-order transition surfaces (a) and lines [(b) and (c)]. N_1 and N_2 are four-phase points. (d) Phase diagram under applied field E in the (a, α, E) space for $\gamma_1 > 0$. Phases II, III, and IV are stable only in the plane $E = 0$. (e) Configuration of two nearest neighbor molecules, used for working out Eq. (8).

V in the three-dimensional space (E, a, α) . The two phases can be reached from the parent SmA phase across second-order transitions. Furthermore, two remarkable field effects can be inferred from the properties of the system under an applied field:

(1) Starting at zero field from the SmC*-type configuration II ($\Psi = 0, \pi$) and applying an increasing longitudinal field, one obtains the sequence of stable configurations II \rightarrow V \rightarrow I. Along this sequence the polarization \vec{P} rotates continuously from $\Psi = 0$ (or π) to $\Psi = \frac{\pi}{2}$ (or $-\frac{\pi}{2}$) and there is an unwinding of the helix even in the presence of the longitudinal field. Hence, under an alternating, positive and negative, longitudinal field the system will exhibit a three-state switching of \vec{P} , with the successive orientations $\Psi = \frac{\pi}{2}, 0$, and $-\frac{\pi}{2}$.

(2) Starting at zero field from the transversely polarized SmA-type phase III ($\xi = 0, P \neq 0$) the application of a longitudinal field will drive the system to a tilted configuration ($\xi \neq 0, P \neq 0$) corresponding to phase I ($\Psi = \pm \frac{\pi}{2}$). This tilt induced by the field corresponds to a *longitudinal electroclinic effect*. Analogously, starting from the tilted SmC-type configuration IV ($\xi \neq 0, P = 0$), the application of E will induce a transverse as well as a longitudinal polarization, with $\Psi = \pm \frac{\pi}{2}$, reflecting a nonlinear piezoelectric effect.

In summary, it has been shown that due to the bent geometry of the molecules, the tilt and polar instabilities may combine to break the achiral symmetry of a SmA configuration in different ways, giving rise to SmC or SmC*-type configurations, but also to an unusual transversely polarized SmA-biaxial configuration or to longitudinally polarized configurations. These latter configurations break the up-down symmetry of the layers but not the $\hat{n} \rightarrow -\hat{n}$ symmetry. When a longitudinal electric field is applied, only the configurations displaying a longitudinal polarization remain stable. This results in a number of new field effects, such as a three-state switching of the transverse polarization under an alternating field, and a longitudinal electroclinic effect.

At last, let us discuss for the stable configuration III the connections existing between the molecular shape, the phenomenological parameters used in our model, and the possible onset of a spontaneous polarization in achiral systems with bent-shaped molecules. Taking each bent molecule as formed by two rigidly connected symmetric arms, with a bend angle ζ [Fig. 2(e)], and assuming a uniaxial nematic-type interaction between the rodlike arms of nearest neighbor molecules, one can write the orientational part of the Hamiltonian for molecules within a smectic layer as

$$H = - \sum_{\substack{\langle \vec{r} \vec{r}' \rangle \\ \vec{r} \neq \vec{r}'}} \sum_{\alpha\beta} J_{\alpha\beta} (|\vec{r} - \vec{r}'|) [\hat{a}_\alpha(\vec{r}) \cdot \hat{a}_\beta(\vec{r}')]^2, \quad (7)$$

where the sum is taken over nearest neighbor pairs. $\alpha, \beta = 1, 2$ denote the two arms of a molecule, and $\hat{a}_\alpha(\vec{r})$ represents a unit vector along the α arm of a molecule at position \vec{r} . Neglecting the off diagonal terms of the interaction strength which are small with respect to the diagonal terms and assuming $J_{\alpha\beta}$ to be isotropic with respect to $|\vec{r} - \vec{r}'|$ and α, β , one gets

$$H = -J \{ 2 \sin^4 \zeta \cos^2 [\varepsilon(\vec{r}) - \varepsilon(\vec{r}')] + \sin^2 2\zeta \cos [\varepsilon(\vec{r}) - \varepsilon(\vec{r}')] \}, \quad (8)$$

where $\varepsilon(\vec{r})$ and $\varepsilon(\vec{r}')$ are the azimuthal angles of the bend directions of the molecules at \vec{r} and \vec{r}' [Fig. 2(e)]. Equation (8) reveals that for $0 < \zeta < \pi/4$ the ground state corresponds to a transversely polarized biaxial SmA phase, whereas for $\pi/4 < \zeta < \pi/2$ a metastable biaxial phase with no transverse polarization also exists. Thus, for small values of ζ the first term inside the braces in Eq. (8) can be neglected, and H reduces to the usual 2D-XY Hamiltonian, in which the interaction strength depends on ζ as $\sim \sin^2 2\zeta$ and therefore reaches a maximal value for $\zeta = 45^\circ$. Accordingly, this 2D model predicts at finite temperature a Kosterlitz-Thouless-type transition [6] from a disordered SmA phase to a transversely polarized SmA phase. In our approach a measure of the molecular bend in the configuration III is given by the magnitude of the transverse polarization $P_t = \pm (\frac{-\alpha}{\beta})^{1/2}$. Actually, P_t expresses the sum of two contributions: the orientational fluctuations of the bend direction of the molecules within a layer, which has been taken into account in Eq. (7), and a contribution depending on the nature and curvature of the molecules. Taking as usual $\alpha = \alpha_o(T - T_c)$, where α_o , as β , is a positive constant and T_c is the transition temperature, one gets $T_c = T + \frac{\beta}{\alpha_o} P_t^2 \sim \sin^2(2\zeta)$, which provides a relationship between the bend angle ζ and the phenomenological parameters.

Fundação de Amparo à Pesquisa do Estado de São Paulo supported this work.

*On leave from the University of Amiens, Amiens, France.

- [1] T. Niori *et al.*, J. Mater. Chem. **6**, 1231 (1996).
- [2] D. R. Link *et al.*, Science **278**, 1924 (1997).
- [3] R. Macdonald *et al.*, Phys. Rev. Lett. **81**, 4408 (1998); A. Jáklí *et al.*, Phys. Rev. E **57**, 6737 (1998).
- [4] R. B. Meyer *et al.*, J. Phys. (Paris) **36**, L-69 (1975).
- [5] A. Roy and N. V. Madhusudana, Europhys. Lett. **39**, 335 (1997).
- [6] J. M. Kosterlitz and D. J. Thouless, J. Phys. C **5**, L124 (1972).